



Citation for published version:

De Paola, A, Trovato, V, Angeli, D & Strbac, G 2019, Value of thermostatic loads in energy frequency response markets: A mean field game approach. in *2019 IEEE Milan PowerTech, PowerTech 2019*. 2019 IEEE Milan PowerTech, PowerTech 2019, IEEE, IEEE Milan PowerTech, Milan, Italy, 23/06/19.
<https://doi.org/10.1109/PTC.2019.8810683>

DOI:

[10.1109/PTC.2019.8810683](https://doi.org/10.1109/PTC.2019.8810683)

Publication date:

2019

Document Version

Peer reviewed version

[Link to publication](#)

© 2019 IEEE. Personal use of this material is permitted. Permission from IEEE must be obtained for all other users, including reprinting/ republishing this material for advertising or promotional purposes, creating new collective works for resale or redistribution to servers or lists, or reuse of any copyrighted components of this work in other works.

University of Bath

Alternative formats

If you require this document in an alternative format, please contact:
openaccess@bath.ac.uk

General rights

Copyright and moral rights for the publications made accessible in the public portal are retained by the authors and/or other copyright owners and it is a condition of accessing publications that users recognise and abide by the legal requirements associated with these rights.

Take down policy

If you believe that this document breaches copyright please contact us providing details, and we will remove access to the work immediately and investigate your claim.

Value of Thermostatic Loads in Energy/Frequency Response Markets: a Mean Field Game Approach

Antonio De Paola
University of Bath
a.de.paola@bath.ac.uk

Vincenzo Trovato
EDF Energy R&D UK and
Imperial College London

David Angeli
Imperial College London and
University of Florence

Goran Strbac
Imperial College London

Abstract—This paper studies the distributed coordination of large populations of thermostatically controlled loads (TCLs). It is assumed that each TCL operates in an integrated energy/frequency response market and reacts to broadcast prices in order to minimize its energy cost and, at the same time, maximize its revenues from frequency response. A mean field game is used to model the competing interactions between the TCLs, quantify their impact on the system unit commitment and characterize the desired market equilibrium solution. This approach is then compared with a no-flexibility case in a 2030 scenario of the GB system, assessing the potential benefits of different types of flexible price-responsive TCLs in terms of cost reduction for the individual customers and for the overall system.

I. INTRODUCTION

One of the defining element of the power system transition towards the smart grid paradigm is an increased flexibility on the demand side. It is envisioned that, in the near future, customers will have the possibility to become “prosumers” and use new technologies such as EVs and smart appliances to actively participate to system operation, exchanging energy and providing ancillary services to the grid [1]. The potential benefits of this innovative setup would include reduced costs for the system (for example through a more efficient integration of renewables) and lower electricity tariffs for the users.

Thermostatically-controlled loads are considered as one of the key technologies to achieve this paradigm shift and a substantial amount of research has investigated system-level coordination of TCLs in multiple contexts, such as energy arbitrage [2] or frequency response (FR) [3].

In particular, competitive paradigms have drawn increasing attention for their capability of preserving customers’ privacy and maximizing their local objectives. With these approaches, each TCL is modelled as a self-interested entity that responds to price signals and determines its operational strategy in order to strike the best trade-off between the electricity cost and the comfort of its individual user. Two main paradigms are usually considered for competitive coordination of flexible loads:

1) *Market-based* [4], [5], [6]: the loads respond autonomously to market prices. These are generated through the resolution of a unit commitment/generation scheduling problem that accounts for the impact of flexible demand.

2) *Game-theoretic* [7], [8], [9]: a more analytical framework is adopted and the interactions between loads are described by a competitive game. Using simplified pricing structures, convergence and optimality of the proposed control schemes are ensured.

This paper aims at bridging the gap between these two research streams to provide new insights on the potential value of TCLs’ flexibility in a competitive setting. As in previous market-based studies, the analysis considers a unit commitment problem with inertia-dependent frequency constraints to characterize system operation, generating relevant price signals that account for multiple generation technologies. At the same time, a game-theoretic formulation is used to analytically characterize the market solution. Differently from previous approaches, a mean field game (MFG) is used to describe the price elasticity of demand and characterize the self-interested choices of the single devices, expressing the resulting market equilibrium as a fixed point of two coupled partial differential equations (PDEs).

With respect to previous applications of MFG in a power system context (e.g for storage [10] or electric vehicles [11]) this paper considers additional relevant elements. On the basis of the framework presented in [12], the proposed formulation envisages TCLs that provide ancillary services in addition to pursuing energy-cost minimization, responding to meaningful price signals generated by a unit commitment problem.

This mathematical formulation is used to quantify the potential value of TCLs flexibility. The energy costs of flexible TCLs operating in an integrated energy/FR market are compared with the business-as-usual, no-flexibility scenario in which the operation of the thermostatic loads is purely driven by their internal temperature. This analysis has been made for eight distinct types of TCLs, considering different penetration rates of flexible device and thus evaluating the impact of competition on the potential cost savings of the devices. Simulation results are presented and discussed for a 2030 scenario of the GB system with large penetration of flexible TCLs and renewables.

The rest of the paper is structured as follows: Section II introduces the considered unit commitment problem and models the population of flexible TCLs. The MFG formulation is presented in Section III and numerically solved in Section IV for a case study of the GB system. Finally, Section V contains some conclusive remarks.

II. MODELLING

The proposed modelling framework can be described by two distinct but interconnected elements, represented in Fig. 1. The population of TCLs responds to two price signals p and ρ and its overall behaviour can be summarised by two quantities U^{TCL} and R^{TCL} . In turn, the resolution of a unit commitment (UC) problem takes into account U^{TCL} and R^{TCL} to determine the generation scheduling decisions and return the price signals p and ρ . Each of the two modelling blocks is now described in detail.

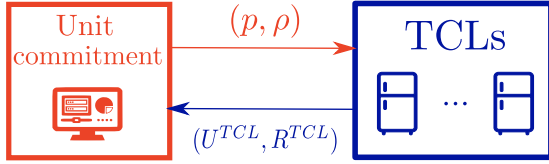


Fig. 1. Interactions between TCLs and unit commitment.

A. Unit Commitment

The UC problem determines the scheduling of the different generation units (in terms of energy and FR) in order to minimize the short-term operating costs of the system. The result of the UC corresponds to the outcome of a centralized market mechanism for energy and FR, if one assumes inelastic demand and perfect competition [13]. Within this framework, the signals p and ρ , which are used to coordinate the TCLs, correspond respectively to the prices of energy and FR.

To simplify the analysis, a Linear Programming formulation has been chosen for the UC problem. It is assumed that, for each generation technology τ , the capacity of the individual generation unit is significantly smaller than the total installed capacity G_τ^{max} . As a result, the commitment decisions can be expressed through a continuous variable $H_\tau(t) \in [0, 1]$, which represents the percentage of $G_\tau^{\text{max}}(t)$ that is on-line at time t . This approach significantly reduces computational times with respect to binary UC and MILP UC. At the same time, it accounts for the fundamental system-level scheduling requirements, i.e. generation-demand balancing and allocation of sufficient frequency-related control to deal with fault events.

For consistency with the mean field game characterization of the TCLs' behaviour, a continuous-time formulation is proposed for the UC problem, which is solved over the time interval $[0, T] \subset \mathbb{R}$. Moreover, inter-temporal constraints such as generation ramping have been neglected, allowing to solve the UC problem on an instant-by-instant basis.

To formally characterize the UC problem, let N_τ denote the number of generation technologies available in the system. The on-line generation (as fraction of total installed/available capacity), the generated power and the allocated response of technology τ at time t are denoted by $H_\tau(t)$, $G_\tau(t)$ and $R_\tau(t)$, respectively. This notation can be extended to consider the vectors $\mathbf{H}(t) = [H_1(t), \dots, H_{N_\tau}(t)]$, $\mathbf{G}(t) = [G_1(t), \dots, G_{N_\tau}(t)]$ and $\mathbf{R}(t) = [R_1(t), \dots, R_{N_\tau}(t)]$. If one denotes by $U^{\text{TCL}}(t)$ and $R^{\text{TCL}}(t)$ the total power consumption and allocated response

of the TCL population, the UC at time t can be expressed as the following optimization problem:

$$\begin{aligned} & \varphi(U^{\text{TCL}}(t), R^{\text{TCL}}(t)) = \\ & \min_{\mathbf{H}(t), \mathbf{G}(t), \mathbf{R}(t)} \sum_{\tau=1}^{N_\tau} c_{1,\tau} \cdot H_\tau(t) G_\tau^{\text{max}}(t) + c_{2,\tau} \cdot G_\tau(t) + c_{3,\tau} \cdot G_\tau^2(t) \end{aligned} \quad (1)$$

with $c_{1,\tau}$ [£/MWh] as no-load cost, $c_{2,\tau}$ [£/MWh] and $c_{3,\tau}$ [$\text{£/MW}^2\text{h}$] as production costs. The objective function (1) corresponds to total generation costs per unit of time and is minimized under the following constraints:

$$\sum_{\tau=1}^{N_\tau} G_\tau(t) - \bar{U}(t) - U^{\text{TCL}}(t) = 0 \quad (2a)$$

$$0 \leq H_\tau(t) \leq 1 \quad \forall \tau \in \{1, \dots, N_\tau\} \quad (2b)$$

$$R_\tau(t) \leq r_\tau \cdot H_\tau(t) \cdot G_\tau^{\text{max}}(t) \quad \forall \tau \in \{1, \dots, N_\tau\} \quad (2c)$$

$$R_\tau(t) \leq s_\tau \cdot [H_\tau(t) \cdot G_\tau^{\text{max}}(t) - G_\tau(t)] \quad \forall \tau \in \{1, \dots, N_\tau\} \quad (2d)$$

$$\mu \cdot r_\tau \cdot H_\tau(t) \cdot G_\tau^{\text{max}}(t) \leq G_\tau(t) \quad \forall \tau \in \{1, \dots, N_\tau\} \quad (2e)$$

$$2\Delta G_L \cdot t_{\text{rcf}} \cdot t_d - t_{\text{rcf}}^2 \cdot \hat{R}(t) - 4\Delta f_{\text{rcf}} \cdot t_d \cdot \hat{H}(t) \leq 0 \quad (2f)$$

$$\bar{q}(t) - \hat{H}(t) \cdot \hat{R}(t) \leq 0 \quad (2g)$$

$$\Delta G_L - D[\bar{U}(t) + U^{\text{TCL}}(t) - R^{\text{TCL}}(t)]\Delta f_{\text{qss}}^{\text{max}} - \hat{R}(t) \leq 0 \quad (2h)$$

Condition (2a) balances supply with demand, which is given by the system inelastic demand $\bar{U}(t)$ plus the total power consumption $U^{\text{TCL}}(t)$ of the TCLs. The inequalities in (2b) follow from the definition of H_τ as percentage of on-line generation. The response R_τ allocated by each technology τ is bounded by the headroom $r_\tau \cdot H_\tau(t) \cdot G_\tau^{\text{max}}(t)$ in (2c) and by the slope s_τ linking the FR with the dispatch level in (2d). In order to prevent trivial solutions with large FR and zero generation, constraint (2e) imposes that the generation dispatch $G_\tau(t)$ must be μ times higher than the maximum available FR.

The constraints (2f)-(2h) ensure secure frequency deviations following an unexpected generation loss ΔG_L . In particular, as demonstrated in [14]:

- *Constraint (2f):* RoCoF condition $\Delta f(t_{\text{rcf}}) \geq \Delta f_{\text{rcf}}$.
- *Constraint (2g):* frequency nadir condition $\Delta f_{\text{nad}} \geq \Delta f_{\text{max}}$ (see [14] for the chosen linearization technique).
- *Constraint (2h):* quasi steady-state frequency condition $\Delta f(t \rightarrow \infty) \geq \Delta f_{\text{qss}}^{\text{max}}$.

For compactness of notation, we have denoted as $\hat{R} = \sum_{\tau=1}^{N_\tau} R_\tau(t) + R^{\text{TCL}}(t)$ the aggregate system FR and by $\hat{H}(t) = \sum_{\tau=1}^{N_\tau} \frac{h_\tau \cdot H_\tau \cdot G_\tau^{\text{max}} - h_L \Delta G_L}{f_0}$ the post-fault inertial response (IR). Relevant quantities in the above expressions include the nominal frequency f_0 , the load damping coefficient D , the inertia constant h_τ of technology τ and the inertia h_L of the infeed generation loss (no longer supporting the system).

The solution φ of the UC problem (1)-(2) has been characterized as a minimized cost, parametrized by U^{TCL} and R^{TCL} . These quantities depend on the operation of the TCLs and do not represent decision variables under the chosen paradigm.

The sensitivity of the optimal solution with respect to these parameters can be expressed by the following two quantities:

$$p(t) = \left. \frac{\partial \varphi(U, R)}{\partial U} \right|_{\substack{U=U^{\text{TCL}}(t) \\ R=R^{\text{TCL}}(t)}} \quad \rho(t) = \left. \frac{\partial \varphi(U, R)}{\partial R} \right|_{\substack{U=U^{\text{TCL}}(t) \\ R=R^{\text{TCL}}(t)}} \quad (3)$$

Note that p can be interpreted as the marginal cost of accommodating an additional unit of power demand and it corresponds to the electricity price. Similarly, ρ represents the marginal saving of allocating one less unit of FR (which would be provided by the TCLs instead). As a result, ρ is the availability fee awarded to the TCLs for FR allocation. Consistently with Fig. 1, these price signals are broadcast to the TCLs, which respond by minimizing their associated costs.

B. Thermostatically controlled loads

The individual TCL is described by the dynamics of its internal temperature T :

$$\dot{T}(t) = f(T(t), u(t)) = -\frac{1}{\sigma} (T(t) - T_{OFF} + \zeta u(t)) \quad (4a)$$

where σ is the TCL thermal time constant, T_{OFF} is the ambient temperature and ζ incorporates the physical model of heat exchange (with $T_{off} - \zeta u(t)$ indicating the asymptotic cooling temperature). An initial temperature $T(0) = \tilde{T}$ is considered. Each TCL can control its instantaneous power consumption $u(t)$, which can take two values: $u(t) = u_{ON}$ (if TCL is ON) and $u(t) = 0$ (if TCL is OFF).

The dynamic modelling is extended through an additional state variable $I(t) = T(t) - \tilde{T}$ that keeps track of the total temperature variation of the TCL over the time interval $[0, t]$. The evolution in time of I is straightforward to characterize:

$$\dot{I}(t) = \dot{T}(t) \quad (5a) \quad I(0) = 0. \quad (5b)$$

The quantity $I(t)$ allows to distinguish multiple TCLs that, at some time t , have reached the same temperature $T(t)$ from different initial values \tilde{T} . This can ensure anti-synchronization of the coordination strategy, as the I tracking cost term presented at the end of this section can diversify the behaviour of the TCLs with equal temperatures.

Under the proposed modelling framework, each TCL can contribute to FR. At any time t , the maximum amount of FR $r(t)$ that can be provided by a single TCL will depend on its power consumption $u(t)$ and internal temperature $T(t)$, according to the following relationship:

$$r(T(t), u(t)) = \lambda(T(t)) \cdot u(t). \quad (6)$$

The individual TCL can provide FR only if it is ON ($u(t) = u_{ON} > 0$) and it is therefore available to reduce its power consumption in case of a frequency event. The decreasing function $\lambda : [T_{MIN}, T_{MAX}] \rightarrow [0, 1]$ in (6) is a weighting term that accounts for the current temperature of the TCL and ensures that a potential FR provision (with the TCL being OFF for some time and increasing its internal temperature) does not lead to undesirable temperature values. For simplicity, in the current analysis $\lambda(T)$ has been chosen as the linear function $\lambda(T) = (T - T_{MAX}) / (T_{MIN} - T_{MAX})$.

An agent-based approach is now considered for the flexible TCLs, which are modelled as selfish rational agents. They autonomously determine their power consumption profile u in response to the broadcast price signals p and ρ in order to minimize their own individual cost J defined below:

$$J(u(\cdot)) = \int_0^{t_{FIN}} p(t) \cdot u(t) - \rho(t) \cdot r(T(t), u(t)) + \alpha(T(t) - \bar{T})^2 + \beta(I(t) - \bar{I}(t))^2 dt + \Psi(I(t_{FIN})), \quad (7)$$

$$\text{subject to: } T(t) \in [T_{MIN}, T_{MAX}] \quad \forall t \in [0, t_{FIN}] \quad (8)$$

where T_{MIN} and T_{MAX} are the operational temperature bounds of the considered TCL.

Each term in (7) is now described in detail:

- *Electricity cost* $p(t) \cdot u(t)$: instantaneous cost associated to the power consumption $u(t)$.
- *Response revenue* $\rho(t) \cdot r(T(t), u(t))$: availability fee awarded for FR provision. It corresponds to the product of the response price ρ and the allocated FR $r(T(t), u(t))$.
- *T tracking cost* $\alpha(T(t) - \bar{T})^2$: discomfort term that penalizes deviations from some target temperature \bar{T} .
- *I tracking cost* $\beta(I(t) - \bar{I}(t))^2$: quadratic cost for deviations of state I from a target signal $\bar{I}(t)$. The purpose of this term is to differentiate the behaviour of TCLs. Multiple loads with equal temperatures $T(t)$ but different initial temperature $T(0) = \tilde{T}$ will adopt different strategies, according to their different state variables $I(t) = T(t) - \tilde{T}$. This allows to avoid undesired synchronization in the proposed coordination algorithm.
- *Terminal cost* $\Psi(I(t_{FIN}))$: used to impose periodic constraints. For example, setting $\Psi(I) = \Lambda \cdot I^2$, the TCLs are incentivized to have $I(t_{FIN}) = T(t_{FIN}) - \tilde{T} = 0$ (equal initial and final temperature).

III. MEAN FIELD GAME FORMULATION

As previously discussed, each TCL determines independently its power consumption profile $u(t)$ – and consequently its allocated FR $r(T(t), u(t))$ – in order to minimize its cost function J , on the basis of the prices p and ρ . By doing so, the population of TCLs will impact the solution φ of the UC problem in (1) through the aggregate quantities U^{TCL} and R^{TCL} , thus modifying the prices p and ρ initially considered. In other words, the TCLs are rational players that compete between each other for power consumption (and FR provision) at times with low prices p (and high prices ρ). The objective of this section is to model these gaming interactions and characterize an equilibrium solution where no TCL has interest in unilaterally modifying its power consumption.

The optimal behaviour and dynamics of the TCLs are described in a mean field game framework by two coupled partial differential equations (PDEs). Denoted by $L(t, u, T, I)$ the argument of the integral in (7), we consider:

- 1) An HJB equation (integrated backward in time), describing the value function associated to (7):

$$-V_t(t, T, I) = \min_{u \in \{0, P_{ON}\}} L(t, u, T, I) + (V_T(t, T, I) + V_I(t, T, I))f(T, u) \quad (9)$$

and the resulting optimal control of the TCLs:

$$u^{\text{FF}}(t, T, I) = \underset{u \in \{0, P_{\text{ON}}\}}{\text{argmin}} L(t, u, T, I) + (V_T(t, T, I) + V_I(t, T, I))f(T, u) \quad (10)$$

2) A transport equation which characterizes the evolution in time of the state distribution m when u^{FF} is applied:

$$m_t(t, T, I) = -[m(t, T, I)f(t, u^{\text{FF}}(t, T, I))]_T - [m(t, T, I)f(T, u^{\text{FF}}(t, T, I))]_I \quad (11)$$

More details on the meaning of V and m and the derivation of the PDEs can be found in [12].

The total power consumption and total allocated FR of the TCLs can now be expressed as the weighted integral (over all feasible state values) of the state distribution m , multiplied by the optimal feedback control strategy u^{FF} . Denoted by N the number of considered devices, it holds:

$$U^{\text{TCL}}(t) = U^{\text{FF}}(t) = N \int_{I_{\text{MIN}}}^{I_{\text{MAX}}} \int_{T_{\text{MIN}}}^{T_{\text{MAX}}} u^{\text{FF}}(t, T, I) m(t, T, I) dT dI \quad (12a)$$

$$R^{\text{TCL}}(t) = R^{\text{FF}}(t) = N \int_{I_{\text{MIN}}}^{I_{\text{MAX}}} \int_{T_{\text{MIN}}}^{T_{\text{MAX}}} r(T, u^{\text{FF}}(t, T, I)) m(t, T, I) dT dI. \quad (12b)$$

It should be emphasized that the PDEs describing the mean field game are coupled: equation (11) depends on the value function V in (9) through u^{FF} in (10). Conversely, the solution m of (11) affects through (12) the values of U^{TCL} and R^{TCL} in (3), thus implicitly changing the price signals p and ρ in (9). The desirable outcome of the coordination of the flexible price-responsive TCLs can then be expressed as a fixed point for equations (1) - (3), (9) - (12), which represents a stable market equilibrium solution. All TCLs apply their best response strategy in response to the price signals p and ρ and, by doing so, their aggregate quantities U^{TCL} and R^{TCL} induce those very same price signals in the unit commitment problem.

IV. ASSESSMENT OF FLEXIBILITY VALUE

In order to assess the value of TCLs' flexibility, the stable market equilibrium characterized in the previous section has been calculated numerically and it is hereby referred to as the Full-Flexibility (FF) scenario. This is compared with the No-Flexibility (NF) scenario, where each TCL pursues normal operation and switches ON and OFF according to its internal temperature, with no impact from prices. In the rest of this section, after a preliminary discussion on the characterization and calculation of these scenarios, the results for the FF and RF case are compared in a 2030 scenario of the GB system.

A. Full-Flexibility and No-Flexibility Scenarios

It is in general difficult to analytically calculate the solution in closed form for the system of equations (1) - (3), (9) - (12), which corresponds to the FF scenario. For this reason, numerical calculations have been performed, using an iterative resolution scheme where these equations are solved sequentially, using the solution of the previous integration as a starting point for the resolution of the next equation. The iterations are stopped when convergence to a fixed point is

obtained. Details on the numerical integration of the PDEs (9)-(11) can be found in [12].

Regarding the NF scenario, it has been assumed that each TCL operates as usual, switching OFF when the minimum temperature T_{MIN} is reached and switching ON at the maximum temperature T_{MAX} . This can be characterized as:

$$\dot{T}(t) = \begin{cases} f(T(t), u_{\text{ON}}) & \text{if } \dot{T}(t^-) < 0, T(t) > T_{\text{MIN}} \\ f(T(t), 0) & \text{if } \dot{T}(t^-) > 0, T(t) < T_{\text{MAX}} \end{cases} \quad (13)$$

We denote by $u^{\text{NF}}(t, \tilde{T})$ the power consumption at time t of the single TCL with initial temperature $T(0) = \tilde{T}$ when (13) is considered in the NF scenario. Assuming the same initial temperature distribution m_0 considered in the FF scenario, the total power consumption U^{TCL} in the NF case is equal to:

$$U^{\text{TCL}}(t) = U^{\text{NF}}(t) = N \int_{T_{\text{MIN}}}^{T_{\text{MAX}}} u^{\text{NF}}(t, \tilde{T}) \cdot m_0(\tilde{T}) d\tilde{T}. \quad (14)$$

It should be emphasized that, in the present NF scenario, the TCLs do not provide frequency response and therefore $R^{\text{TCL}}(t) = R^{\text{NF}}(t) = 0$.

B. Case study

The FF and NF solutions have been compared in a typical 2030 scenario of the GB system, whose main generation parameters are presented in Table I. Eight types of refrigeration units across the domestic and commercial sectors have been considered. For the domestic sector we distinguish refrigerators, freezers and fridge-freezers, while within the commercial domain we take into account bottle coolers (with glass doors), refrigerators, freezers and two different multideck refrigerators (open retail units). Representative parameters of the thermal models are from [18]. For simulations, we considered $N = 20 \cdot 10^6$ domestic fridge-freezers resulting in a steady state power consumption $U_0 = 790$ MW. The population size N of other classes of TCLs was modified so as to ensure equal steady-state power consumption in all cases. Heterogeneous populations of TCLs will be considered in future work but it is reasonable to assume that, if multiple types of TCLs are considered at once, the result will be a combination of the outcomes for the associated homogeneous scenarios, which are presented below. The simulation parameters, including the ones for the cost function J in (7), have been chosen as in [12]. Simulations have been performed in a MATLAB environment and have required, for each TCL type, about 11 minutes on a HP EliteBook laptop with an Intel(R) i5 CPU (2.60 GhZ) and 8 GB of RAM.

C. Simulation Results

The comparison between the FF and NF scenarios is initially performed in Fig. 2 for the total profiles of TCL power consumption U^{TCL} (U^{FF} and U^{RF} , respectively) and the total FR allocation R^{TCL} (R^{FF} and R^{RF} , respectively). Similarly, Fig. 3 represents the energy prices and the response availability fees in the two scenarios, as obtained from (3). For compactness, Fig. 2 and 3 focus on domestic fridge-freezers, where the iterative algorithm for the FF case converges in 75 iterations. Similar results are obtained for other classes of TCLs.

TABLE I
CHARACTERISTICS OF THERMAL AND WIND GENERATION

| | Nuclear | CCGT | OCGT | Wind |
|----------------------------------------------------|---------|-------|-------|-------|
| Installed capacity G_{τ}^{\max} [MW] | 10000 | 25000 | 20000 | 40000 |
| No-load cost $c_{1,\tau}$ [€/MWh] | 0 | 16 | 17.5 | 0 |
| Production cost $c_{2,\tau}$ [€/MWh] | 2 | 45 | 120 | 1 |
| Production cost $c_{3,\tau}$ [€/MW ² h] | 0.001 | 0.01 | 0.015 | 0.001 |
| Constant of inertia h_{τ} [s] | 6 | 4 | 4 | - |
| FR headroom r_{τ} | - | 0.1 | 0.1 | - |
| FR slope s_{τ} | - | 0.4 | 0.5 | - |

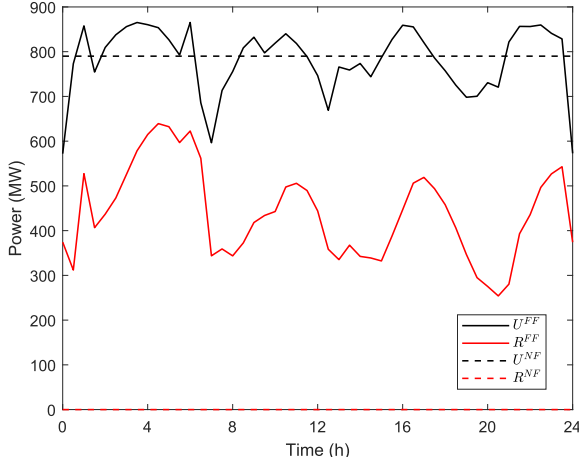


Fig. 2. Total power consumption of the TCLs (black) and allocated response (red), in the FF scenario (continuous lines) and in the NF case (dashed lines).

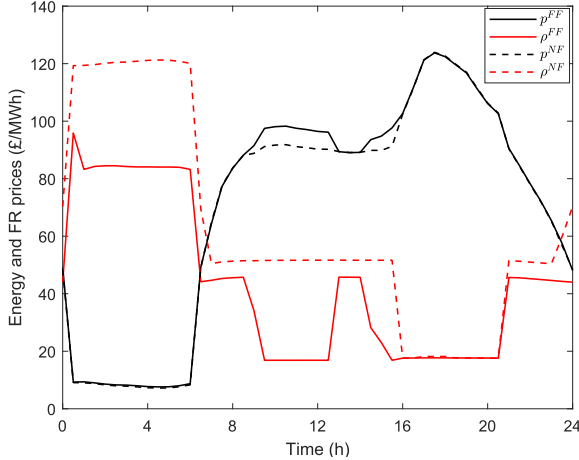


Fig. 3. Electricity price (black) and response availability price (red), in the FF scenario (continuous lines) and in the NF case (dashed lines).

Some preliminary observation can be made regarding the variations over time of the aggregate quantities U^{FF} and R^{FF} , which are strictly related to the price signals p^{FF} and ρ^{FF} . During the early hours of the day, when demand is low, there is high value in FR provision (ρ^{FF} is high) and the electricity price p^{FF} is low. As a result, most of the TCLs will tend to consume power and participate to FR, leading to high values of

U^{FF} and R^{FF} . Conversely, when the prices change significantly at about $t = 6$ h, the aggregate power consumption U^{FF} and allocated response R^{FF} have a sharp decrease. The oscillations of these quantities do not only depend on prices but are also affected by the dynamics of the TCLs and by the sinusoidal function chosen for the reference \bar{I} in (7). Conversely, in the NF scenario, the behaviour of the TCLs is exclusively driven by their internal temperature. The total power U^{NF} in Fig. 2 remains approximatively constant and equal to the steady-state power consumption U_0 . As previously mentioned, in the present case the allocated response R^{NF} is equal to zero.

The value of TCLs' flexibility is now quantified by comparing the daily energy costs sustained by single TCLs in both cases. In the FF scenario, the cost J^{FF} of the single load will correspond to J in (7), evaluated at the optimal solution u^{FF} , with prices $p = p^{\text{FF}}$ and $\rho = \rho^{\text{FF}}$. In the NF scenario, the daily cost will simply correspond to the following energy cost:

$$J^{\text{NF}} = \int_0^{t_{\text{FIN}}} p^{\text{FF}}(t) \cdot u^{\text{NF}}(t, \tilde{T}) dt.$$

The percentage (daily) cost saving J^{S} obtained in the FF case, with $J^{\text{S}} = (J^{\text{NF}} - J^{\text{FF}}) / J^{\text{NF}} \times 100$, is represented in Fig. 4 as a function of the initial temperature \tilde{T} of the single device, for the eight considered types of TCLs. It can be seen that, by

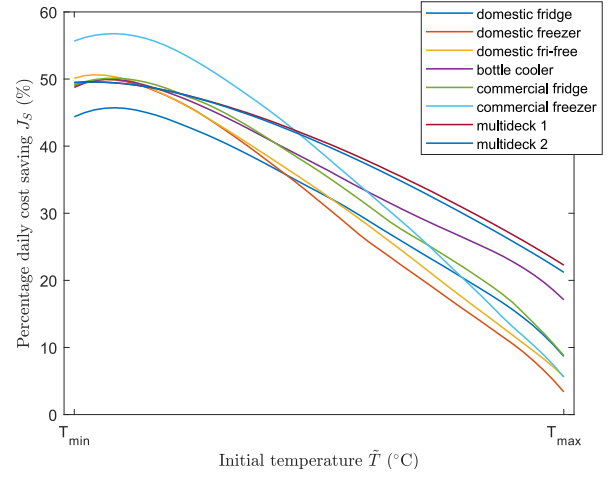


Fig. 4. Daily flexibility cost saving J^{S} , for different types of individual TCLs, as a function of their initial temperature.

exploiting their flexibility, the TCLs can reduce their energy cost on average by 30% in the FF scenario. Note also the higher savings for TCLs that have low initial temperature and can therefore take full advantage of the first hours of the day, with low electricity price p^{FF} and high availability response fee ρ^{FF} , as shown in Fig. 3. The effect of competition between TCLs has also been quantified, assuming that only a fraction of the TCLs population exploits its flexibility and participates in the FF scenario. The resulting daily costs, represented for simplicity only in the case $T(0) = \tilde{T} = T_{\text{MIN}}$ are compared in Fig. 5. As expected, competition between the loads has the effect of decreasing the savings from flexibility: the more

TCLs shift power consumption at times with lower prices, the more the aggregate demand and the prices will increase at those times. Similarly, when more FR is allocated by a larger number of TCLs, its value for the system will decrease and the resulting availability fee ρ awarded for FR will be lower. It is worth pointing out the different magnitude in costs faced by single multidecks and bottle coolers compared to the other appliances. This is due to their large duty cycles ($\approx 0.6-0.7$), caused by a small range of operating temperatures and by the poor level of insulation. The door of a bottle cooler is made by glass (thermal conductivity higher than proper insulation material) while multidecks are open retail units [15]. Moreover, the operating power consumption of a multideck 2 is 12 times higher than the domestic refrigerator (70 W).

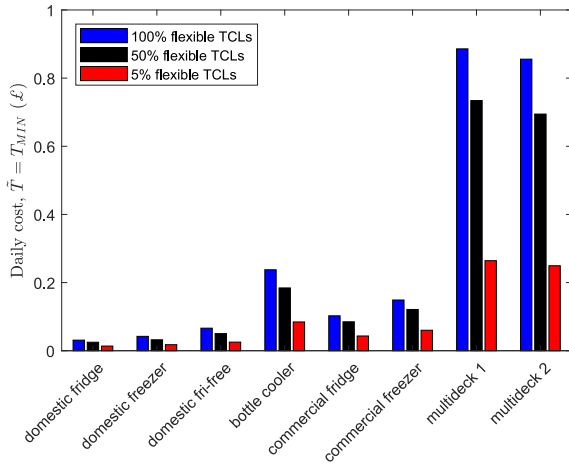


Fig. 5. Daily cost savings for different percentages of flexible TCLs.

Finally, the FF and NF scenarios are compared in terms of total system costs in Fig. 6. In the FF case, two different terms have to be considered: the minimized generation costs φ (red bars) plus the FR availability payment to the TCLs (blue bars), equal to $\int \rho^{\text{FF}}(t)R^{\text{FF}}(t)dt$. As expected, the flexibility of the TCLs in the FF case allows to reduce the generation cost φ by about 3%. A substantial 1% reduction is still obtained once the FR availability payments are also considered.

V. CONCLUSIONS

A distributed price-based strategy is proposed for coordination of flexible TCLs participating to an integrated energy/frequency response market. Under a competitive framework, the loads minimize their operational cost according to broadcast price signals, which are derived from the resolution of a unit commitment problem with inertia-dependent frequency constraints. A mean field game is used to describe the interactions between large populations of TCLs, characterizing the market equilibrium as the fixed point solution of coupled PDEs. The benefits from TCLs flexibility in terms of reduced costs for the appliances and for the system have been quantified through comparisons with a business-as-usual, no-flexibility case, considering a 2030 scenario of the GB system.

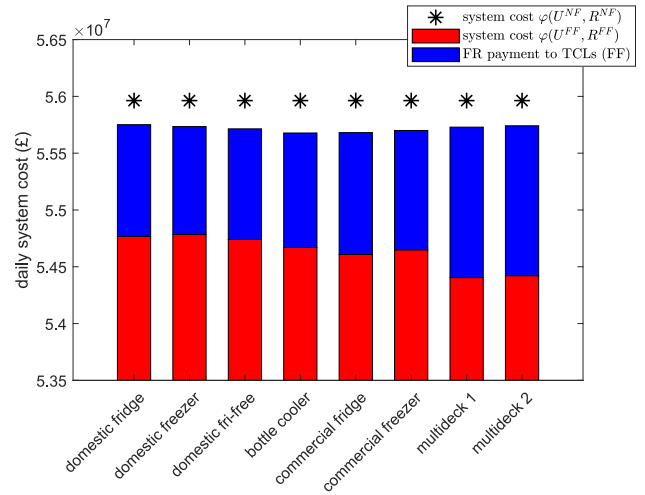


Fig. 6. Daily system costs in the FF and NF case.

REFERENCES

- [1] A. Ipakchi and F. Albuyeh, "Grid of the future," *IEEE Power and Energy Magazine*, vol. 7, no. 2, pp. 52–62, March 2009.
- [2] J. L. Mathieu, M. Kamgarpour, J. Lygeros, G. Andersson, and D. S. Callaway, "Arbitrating intraday wholesale energy market prices with aggregations of thermostatic loads," *IEEE Transactions on Power Systems*, vol. 30, no. 2, pp. 763–772, March 2015.
- [3] Y. Chen, A. Bui, and S. Meyn, "Estimation and control of quality of service in demand dispatch," *IEEE Transactions on Smart Grid*, vol. 9, no. 5, pp. 5348–5356, Sept 2018.
- [4] A. L. Motto, F. D. Galiana, A. J. Conejo, and M. Huneault, "On walrasian equilibrium for pool-based electricity markets," *IEEE Transactions on Power Systems*, vol. 17, no. 3, pp. 774–781, Aug 2002.
- [5] K. Singh, N. P. Padhy, and J. Sharma, "Influence of price responsive demand shifting bidding on congestion and lmp in pool-based day-ahead electricity markets," *IEEE Transactions on Power Systems*, vol. 26, no. 2, pp. 886–896, May 2011.
- [6] A. Khodaei, M. Shahidehpour, and S. Bahramirad, "Scuc with hourly demand response considering intertemporal load characteristics," *IEEE Transactions on Smart Grid*, vol. 2, no. 3, pp. 564–571, Sept 2011.
- [7] L. Gan, U. Topcu, and S. H. Low, "Optimal decentralized protocol for electric vehicle charging," *IEEE Transactions on Power Systems*, vol. 28, no. 2, pp. 940–951, 2013.
- [8] Z. Ma, D. Callaway, and I. Hiskens, "Decentralized charging control of large populations of plug-in electric vehicles," *IEEE Transactions on Control Systems Technology*, vol. 21, no. 1, pp. 67–78, 2013.
- [9] A. De Paola, D. Angeli, and G. Strbac, "Price-based schemes for distributed coordination of flexible demand in the electricity market," *IEEE Trans. on Smart Grid*, vol. 8, no. 6, pp. 3104–3116, Nov 2017.
- [10] —, "Distributed control of micro-storage devices with mean field games," *IEEE Transactions on Smart Grid*, vol. 7, no. 2, pp. 1119–1127, March 2016.
- [11] Z. Zhu, S. Lambetharan, W. H. Chin, and Z. Fan, "A mean field game theoretic approach to electric vehicles charging," *IEEE Access*, vol. 4, pp. 3501–3510, 2016.
- [12] A. De Paola, V. Trovato, D. Angeli, and G. Strbac, "A mean field game approach for distributed control of thermostatic loads acting in simultaneous energy-frequency response markets," *IEEE Transactions on Smart Grid*, pp. 1–1, 2019.
- [13] D. Papadaskalopoulos and G. Strbac, "Decentralized participation of flexible demand in electricity markets - part i: Market mechanism," *IEEE Trans. on Power Syst.*, vol. 28, no. 4, pp. 3658–3666, Nov 2013.
- [14] V. Trovato, A. Bialecki, and A. Dallagi, "Unit commitment with inertia-dependent and multi-speed allocation of frequency response services," *IEEE Transactions on Power Systems*, 2018 (in press).
- [15] V. Trovato, S. H. Tindemans, and G. Strbac, "Leaky storage model for optimal multi-service allocation of thermostatic loads," *IET Generation, Transmission Distribution*, vol. 10, no. 3, pp. 585–593, 2016.